Improvement in the Oxidation Resistance of Ti-6Al-4V Alloy by Sol–gel Derived Al2O3 Film

X. J. Zhang[1],[2*], B. Y. Ren[1], Y. G. Sheng[1] and N. Tsubaki[2]

1. College of Applied Chemistry, Shenyang University of Chemical Technology, Shenyang 110142, China
2. Department of Applied Chemistry, School of Engineering, University of Toyama, Gofuku 3190, Toyama 930-8555, Japan

(Received October 6, 2009: final form October 16, 2009)

ABSTRACT

Alumina coating derived by sol-gel processing was deposited on Ti-6Al-4V alloy by dip-coating technique. Isothermal oxidation and cyclic oxidation at 873 K and 973 K in static air of the coated specimens with different thickness alumina coating and uncoated ones were performed to investigate the effect of the alumina coating on the oxidation behavior of the Ti-6Al-4V alloy by thermogravimetry, SEM and XRD. The present film exhibited a beneficial effect on the cyclic oxidation resistance of the alloy in air. The optimal thickness of the applied coating on the present alloy was determined in terms of the relationship between the average parabolic rate constants of isothermal oxidation and the coating thickness. Severe spallation and stratification of the scales were observed on the blank specimens, but not on the coated ones. The formation of rutile titania layer beneath and above the alumina film indicated that the growth of the multilayered and mixed oxide scales was dominated by both outward diffusion of metal and inward diffusion of oxygen. The possible mechanism of the thin film on the oxidation behavior of the alloy was discussed.

Keywords: Alumina coating; High temperature oxidation; Sol-gel processing; Ti-6Al-4V

1. INTRODUCTION

The two intermetallic compounds α_2-Ti_3Al and γ-TiAl are the most attractive heat-resisting light materials in the area of astronautics and aeronautics /1/. However, their poor oxidation resistance at high temperatures becomes an important obstacle for the application of these materials /2/. Effects of alloying and protective coatings on the improvement of the oxygen-induced embrittlement and oxidation resistance of Ti alloys were widely studied. Alloying elements have been added to binary Ti–Al alloys in order to increase the oxidation resistance /3-5/. The beneficial elements, such as Mo, Nb and W resulted in protective oxidation behavior, while the addition of V to TiAl-based alloy can improve the mechanical properties, but does harm to the oxidation resistant. Many coatings could offer oxidation protectiveness for titanium alloys and act as a barrier to reduce the ingress of oxygen at elevated temperatures /6-10/. Most of the deposited coatings usually have shortcomings of poor adhesion and significant inter-diffusion between the coating and the substrate /11/. Thus, new technologies or new

---

[*] Tel.: +86 24 89383297.
E-mail.: xjzhangsyict@gmail.com

coating system need to be developed in order to further improve the oxidation resistance of Ti–Al-based alloys.

Sol–gel processes have been widely used to prepare various thin films for modifying the properties of surfaces by low temperature treatment without altering the original properties of strength and toughness of the substrates /12, 13/. Coatings derived from the sol-gel route don't require high processing temperatures and high vacuum conditions as in case of CVD and PVD. Further, this process is relatively less expensive, easily adaptable and applicable to coat on material with complex shaped geometry and accessible to produce very small particles - usually in the nano-scale range. In our group, Al_2O_3 thin films /14, 15/, Al_2O_3/ZrO_2 duplex film /16/ and amorphous SiO_2 thin films /17, 18/ have been applied to improve the oxidation resistance of intermetallic compounds α_2-Ti_3Al or γ-TiAl, but its use as a protective coating on the Ti-6Al-4V alloy has not been reported. The aim of the present work is to study the effect of sol-gel-derived Al_2O_3 thin film on the oxidation resistance of the present alloy.

2. EXPERIMENTAL PROCEDURE

The commercial Ti-6Al-4V alloy was cut into specimens with dimensions 12 mm x 10 mm x 1.5 mm using a spark wire machine and their surfaces were grinded to 1200 grit SiC paper. In order to grip the specimens during the dipping coating, a hole with diameter about 2 mm was drilled. Then the samples were degreased ultrasonically in acetone, cleaned by distilled water and dried in air before use.

Al_2O_3 sol was prepared by mixing Al-iso-propoxide ($Al(OC_3H_7)_3$ purity >98%) and water in their molar ratio of 1:150. A small amount of diluted nitric acid was added to maintain the pH about 4. The suspension was refluxed and stirred vigorously at 358 K for several hours until it got converted into a clear sol. The sol was allowed to cool to room temperature /19/. The viscosity of the sol was also measured by using a viscometer which found to be 1.35 mPas. The concentration of solid content in Al_2O_3 form analyzed by chemically gravimetric analysis is about 3.5 mass %.

The specimens were dipped into the Al_2O_3 sol and withdrawn at a rate of 0.01m/min by dip-coating equipment, dried in air for 20 min at room temperature, and then dried at 348 K in a vacuum drying oven for 40 min. Subsequently, heat treatment in argon atmosphere was carried out after repeating 5 times dipping. The level furnace was first evacuated to a pressure of 2 x 10^{-1} Pa and then argon was introduced as a protective gas at a flow rate of 0.5 L/min. The level furnace was then heated up to 423 K at a rate of 5 K/min, kept at the temperature for 1 h, and then heated up to 623 K at the same heating rate and kept the temperature for 1 h, and finally it was heated up to 823 K and kept the temperature for 1 h. The target sol-gel thin films were finally obtained by cooling the specimens to ambient temperature in the furnace. In the present investigation, the sintering was conducted after three dip-coatings. Non-treated samples were also systematically treated in all runs. The hypothetical Al_2O_3 thickness coated on the alloy was calculated in the light of the mass change of the specimens before the dip-coating and after the heat treatment, the surface area of the coated specimens and the alumina density. The specimens were coated by alumina with the thickness of 0.3, 0.5, 0.8 and 1.0 μm by different dip-coating and sintering times in order to gain the optimal thickness of the coating on the oxidation resistance.

Isothermal oxidations were carried out in static air at 873 and 973 K with weight measurements performed at regular intervals. The specimens were placed in Al_2O_3 crucibles, oxidized at desired temperatures in ambient air, and cooled to room temperature at regular intervals of 5–20 h for mass measurement with an electronic balance. Cyclic oxidation was conducted at 873 K and 973 K in air. The specimens were kept in the furnace at desired temperatures for 1 h and then taken out to cool for 15 min in air. This process was defined as one cycle, and the cycle was repeated 80 times at 873K and 30 times at 973 K. An analytical balance with a sensitivity of 10^{-5} g was used to measure the mass of the specimens at intervals during the isothermal and cyclic oxidation tests.

The surface morphologies and cross sections of the oxidized samples were characterized by Scanning Electronic Microscope (SEM) equipped with Energy Dispersive Spectrum (EDS), while the phase compositions of the oxide scales were analyzed using an X-ray diffractometer (XRD) with Cu-Kα radiation.

3. RESULTS

3.1 Characteristics of alumina film

The surface and cross sectional morphologies of the as-fabricated alumina films with a thickness of 0.8 μm on Ti-6Al-4V alloy were examined by SEM, as shown in Figure 1. It was observed that surface morphology of the film was uniform and crack free.

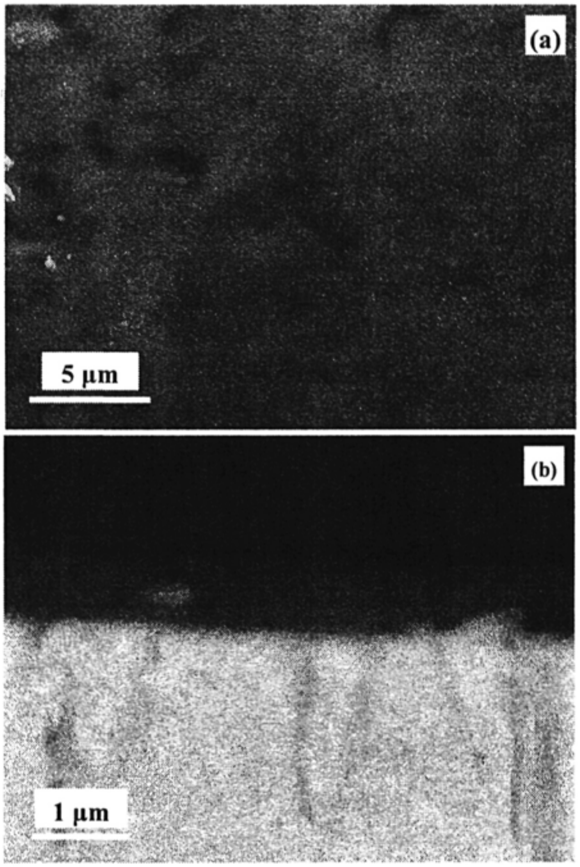

Fig. 1: Top view (a) and cross section (b) of the alumina coating on the Ti-6Al-4V alloy.

The polishing scratch beneath the alumina coating was observed. Since the coatings were multilayered with every three layers fired separately, the most inner layers of the coatings were fired two times, whereas the top layers were fired only once. Therefore, the inner layers are expected to have fewer pores. Even there were pores in the previous fired layers; these pores would be filled at least partially by the subsequent layers of coatings due to the infiltration effect of the sol–gel dipping.

3.2 Optimal thickness of the coating

The specimens with different thickness of alumina were put into the furnace after the desired temperatures reached. The mass gains of the coated specimens with various thick coatings were gained at regular intervals by an analytical balance. The average parabolic rate constant (k_p) could be obtained by a linear fit of $\Delta m/S = k_p t^{1/2} + A$, where S is the sample surface area and A is a constant. The relationship curves of the average parabolic rate constant and the coating thickness at both temperatures are shown in Figure 2. The average parabolic rate constant decreased with the thickness of the coating at both temperatures when the thickness was lower than 0.8 μm. On the contrary, the k_p value increased abruptly and more obvious at 973 K than at 873 K when the thickness of the alumina film exceeded 0.8 μm. It is very clear that the optimal thickness of alumina coating providing the oxidation resistance for the present alloy is about 0.8 μm.

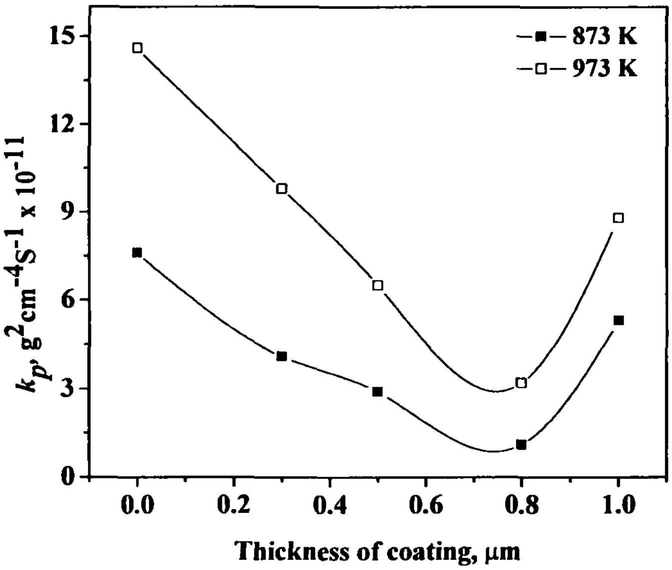

Fig. 2: Relationship curve of average parabolic rate constant with thickness of the coating at 873 and 973 K.

3.3 Oxidation kinetics

The cyclic oxidation kinetics curves of the blank and coated specimens with an alumina thickness of 0.8 μm at 873 K for 80 cycles and 973 K for 30 times in static air are shown in Figure 3. At 873 K, the break-away oxidation occurred on the Ti-6Al-4V alloy after 10 times cycles due to the abrupt increase of the mass gain per unit surface area from 10 h to 20 h. After 50 cycles, large pieces of scale began to spall off, resulting in the mass loss of the specimen. Reversely, the coated specimen had the similar oxidation kinetics to the isothermal oxidation. It can be seen that the mass gain of the coated specimen kept increasing during the cyclic oxidation. The oxide scale formed on the coated specimen did not spall during the whole test, which resulted in a smooth curve. At 973 K, the scale formed on the blank specimens begun to spall off after 16 cycles, while the spallation of the scale did not occur on the coated samples until the test was finished. Cyclic oxidation tests indicated that the Al_2O_3 thin film significantly improved the cyclic oxidation resistance of the alloy at both temperatures in air.

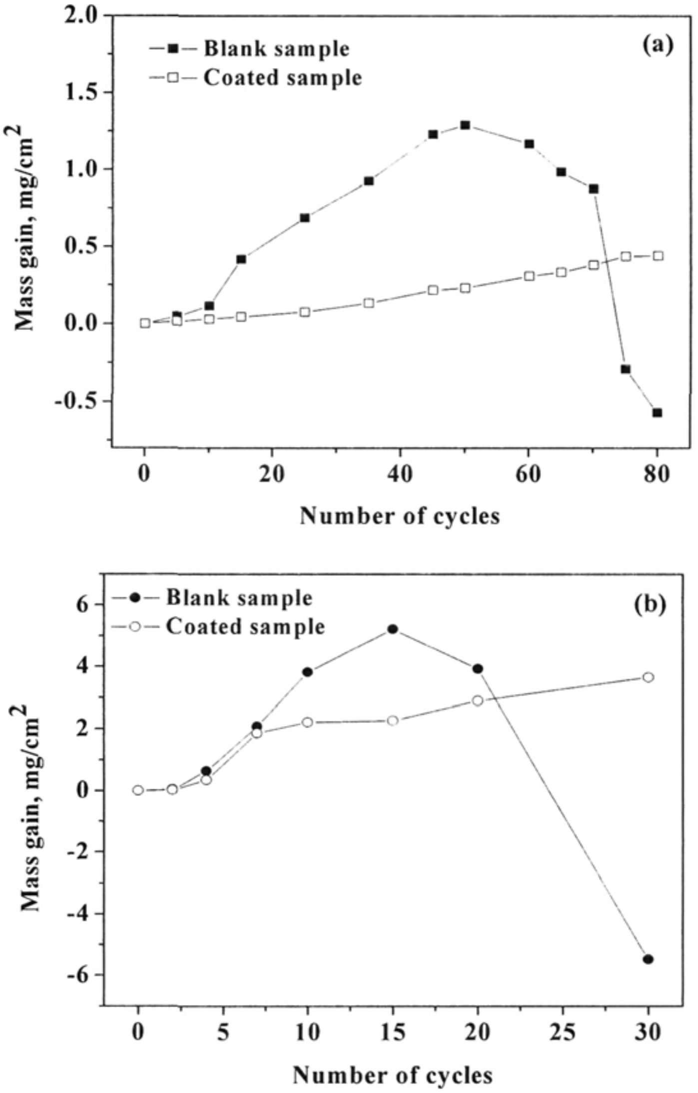

Fig. 3: Cyclic oxidation kinetics curves of the blank and coated samples oxidized in air. (a) 873 K and (b) 973 K.

3.4 Scale composition

The phase compositions from XRD analysis of the oxide scales on the blank and coated specimens oxidized isothermally for 80 h in air at 873 K are shown in Figure 4. TiO_2 (rutile) could be detected in all cases of the specimens after oxidation, but the relative intensity of the TiO_2 peaks on the coated samples (Fig.4b) was weaker than that on the uncoated samples (Fig.4a). The examination reveals that less TiO_2 formed on coated specimens and the growth of TiO_2 on the coated specimens was restrained due to the presence of the alumina thin film. The XRD results revealed that the growth of oxides on the coated specimens was restrained by the presence of the thin film.

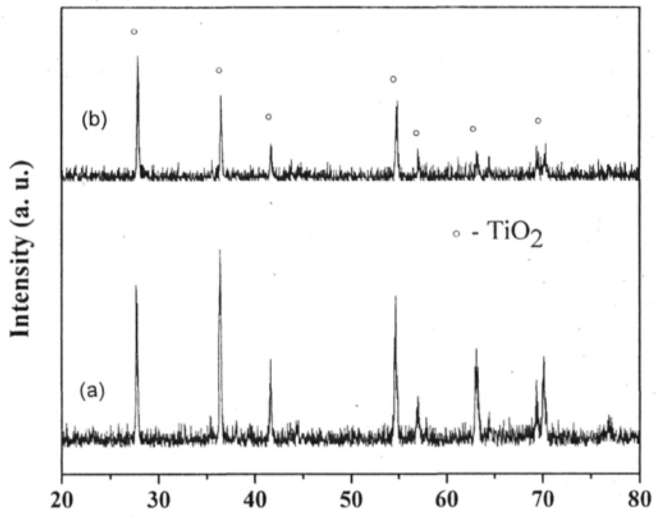

Fig. 4: XRD patterns of the samples oxidized in air for 80h at 873 K. (a) blank sample and (b) coated one.

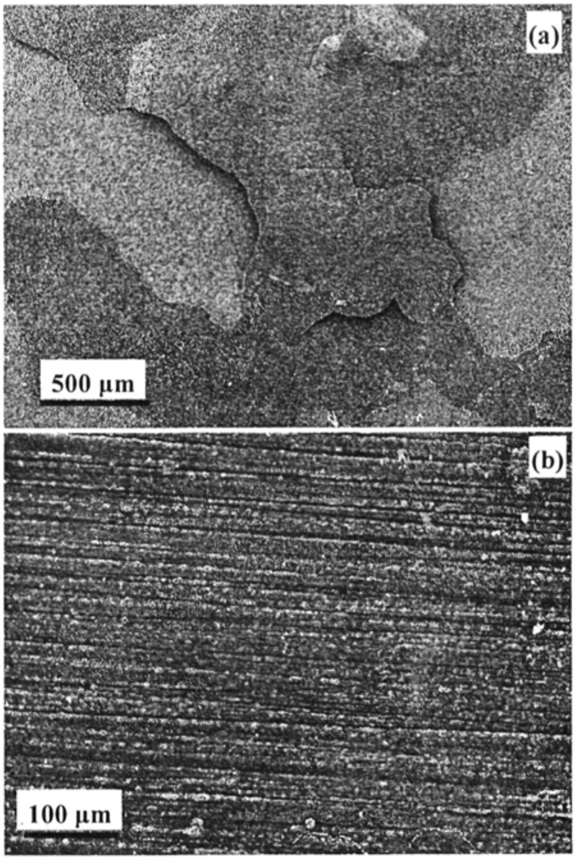

Fig. 5: Surface morphologies of the blank and coated specimens after 80 times cycles at 873 K in air. (a) blank specimen and (b) coated one.

3.5 Scale morphology

Surface morphologies of the scales formed on the specimens oxidized at 873 K for 80 cycles in air are shown in Figure 5. Severe cracking and spallation of the oxide scales were observed on the blank specimens (Fig. 6a), but not on the coated ones. The outmost surface of coated specimen at 873 K was covered by very fine newly-formed oxides. It was likely to be TiO_2 according to EDS analysis on the surfaces. Additionally, the polishing scratch beneath new oxides and the alumina coating could be observed. The oxide scale formed on the surface of the coated specimens at 973 K is quite similar to that observed on specimens oxidized at 873 K.

The cross-sectional morphologies of the specimens after 80 h oxidation at 873 K are shown in Figure 6. The oxide scales on the uncoated specimens were much thicker than those on the coated ones. For uncoated specimens, the thickness of the oxide scale at 873 K was about 40 μm, while that for the coated specimens were about 10 μm. The oxide scales formed on the uncoated specimens were loose and porous, and stratified after 80 h oxidation at 873 K. The layer of TiO_2 and the mixture of minor amount TiO_2 and abundant Al_2O_3 was alternating. For the coated one, the scale was separated by the alumina thin film and the thickness of the two parts was almost same according to the EDS results at the three layers.

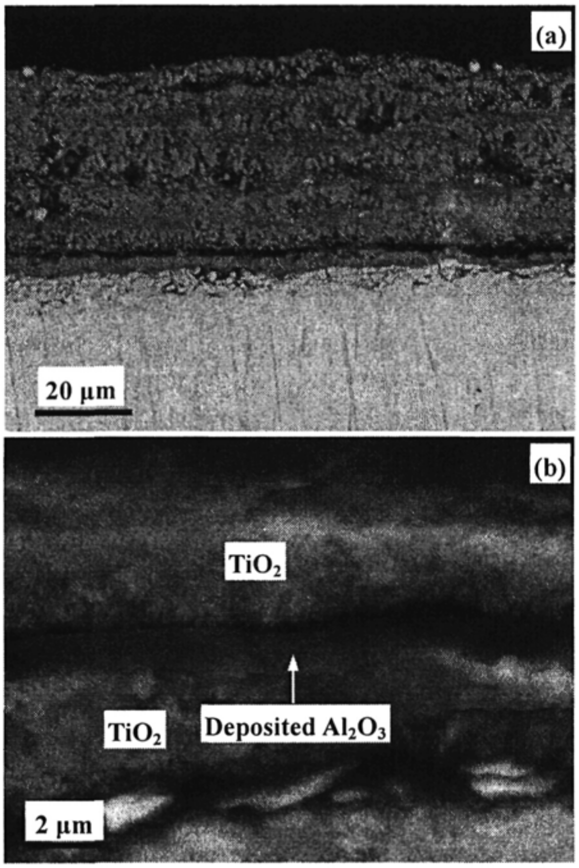

Fig. 6: Cross sectional morphologies of the blank and coated sample after 80 h oxidation at 873 K in static air. (a) blank sample and (b) coated one.

4. DISCUSSION

Stratification of oxide scales on the bare Ti-6Al-4V alloy revealed in the present work is in agreement with previous work /20/. TiO_2 rutile phase mainly forms on the surface of Ti-6Al-4V alloy. Small amount of Al_2O_3 is present in mixture with rutile. At sufficiently high temperatures, oxygen diffuses through the oxide layer, and at the metal–oxide interface, it reacts with titanium to form TiO_2. Formation of oxide layer is accompanied with the dissolution of diffusing oxygen in the metal beneath it. Increasing oxidation temperature accelerates the oxidation rate, allowing formation of thicker oxide layer and deeper oxygen diffusion zone.

Overall the results obtained in the present examination show that sol–gel Al_2O_3 films have beneficial effects on the oxidation resistance of Ti-6Al-4V in air at both temperatures. The present films lead to significant decrease in oxidation rates, elimination of cracking and spallation of the oxide scales during the cyclic oxidation, especially the results obtained from the specimens with a thickness of 0.8 μm. For the bare alloy, inward diffusion of oxygen-ion or outward diffusion of Ti-ion is needed to favor the growth of the oxides. In case of the coated specimens, oxygen has to penetrate through the coating, which may occur either by solid-state diffusion or possibly also by transport along pores, cracks or other physical discontinuities in the coating. In any case, oxygen has a much more restricted access to the scale surface for the coated samples than for the uncoated ones. It does not seem possible to make any quantitative or even semi-quantitative analysis of the effects that a reduction of the oxygen pressure at the external scale surface may have on the kinetics of growth of the two oxides, especially because their defect structure is quite complex and not well understood. In view of the statement, the thicker coating would be good for the oxidation resistance. On the contrary, the optimal thickness of the alumina coating on the Ti-6Al-4V is 0.8 μm when oxidized isothermally and cyclically. In fact, the present isothermal oxidation is also a cyclic behavior due to the discontinuous mass measurement. During the cyclic oxidation, Ti could diffuse outwards and O could diffuse inwards through the coating by solid-state diffusion or possibly also by transport along pores, microcracks caused by the heat treatment or the cyclic behavior in the coating. The film could not act as a better diffusion barrier to prevent the outward diffusion of Ti and the inward diffusion of O when the thickness of the alumina coating is lower than the optimal value. The thicker alumina coating would be cracked during the heat and cool alternation when the thickness of the present coating exceeds the critical value due to the mismatch of the thermal expansion coefficient between the outer sol–gel layer and the substrate, meanwhile, the thicker coatings would become brittle and the stress developed during the oxide growth induces some cracks. Those cracks would act as channels for Ti and O to attack the substrate, as a result of increasing of oxidation rate and spallation of the oxide scale, as the case of 1.0 μm and shown in Fig. 2.

Under standard condition, the values of the Gibbs formation energy for Ti_2O_3 (−1433.824 kJ/mol), which transforms to TiO_2 by further oxidation, and Al_2O_3 (−1582.271 kJ/mol) in the reaction of pure Ti and Al with oxygen respectively are quite close /21/. The equilibrium oxygen partial pressure of TiO_2 is higher than that of Al_2O_3. In previous standpoints /15, 22/, the applied Al_2O_3 coating could lower the oxygen partial pressure between the film and the substrate. In fact, the oxygen pressure for the alloy/TiO_2/Al_2O_3 equilibrium is fixed under constant temperature. In view of the nature, a real possibility is that the effect of the presence of the coating reduces the oxygen pressure available at the scale surface by restricting the availability of oxygen from the gas with respect to the case of the bare alloy. In fact, in the presence of the coating oxygen has to penetrate through the coating. In any case, oxygen has a much more restricted access to the scale surface for the coated samples than for the uncoated ones.

5. CONCLUSIONS

Sol-gel derived Al_2O_3 thin film has been applied on the surface of Ti-6Al-4V alloy. By investigating the isothermal and cyclic oxidation behaviors of the uncoated and coated alloys, the following conclusions can be drawn. The Al_2O_3 thin film had a positive effect on the oxidation resistant of the alloy. The optimal thickness of the Al_2O_3 thin film derived by sol-gel technique was about 0.8 μm. Spallation and cracking of oxide scales on the bare alloy were observed, while they were reduced after the deposition of alumina. The applied thin film reduced the oxygen pressure available at the scale surface by restricting the availability of oxygen from the gas with respect to the case of the bare alloy.

REFERENCES

1. D. J. Dequette and N. S. Stoloff, Key Eng. Mater. 77/78: 289(1993).
2. S. Becker, A. Rahmel, M. Schorr and M. Schütze, Oxid. Met. 38: 425 (1992).
3. A. Rahmel and P. J. Spencer, Oxid. Met. 35: 53(1999).
4. H. R. Jiang, M. Hirohasi, Y. Lu and H. Imanari, Scr. Mater. 46: 639(2002).
5. Y. Shida and H. Anada, Oxid. Met. 45: 197(1996).
6. H. L. Du, P. K. Datta, J. S. Burnell-Gray and G. B. Lewis, J. Mater. Sci. 30: 2640(1995).
7. D. W. Mckee and K. L. Luthra, Surf. Coat. Technol. 56: 109(1993).
8. R. K. Clark, J. Unnan and K. E. Wiedemann, Oxid. Met. 28: 391(1987).
9. S. Fujishiro and D. Eylon, Metall. Trans. Phys. Metall. Mater. Sci. 11A:1259(1980).
10. S. Taniguchi, T. Shibada, T. Yamada, H. Lou, F. Wang and W. Wu, Oxid. Met. 39: 457(1993).
11. M. S. Chu and S. K. Wu, Surf. Coat. Technol. 179: 257(2004).
12. H. Li, K. Liang, L. Mei, S. Gu and S. Wang, Mater. Lett. 51: 320(2001).
13. S. Zhang and W. E. Lee, J. Eur. Ceram. Soc. 23: 1215 (2003).
14. X. J. Zhang, Q. Li, S. Y. Zhao, C. X. Gao, L. Wang and J. Zhang, App. Sur. Sci. 255: 1860 (2008).
15. C. Z. Yu, S. L. Zhu, D. Z. Wei and F. H. Wang, Surf. Coat. Technol. 201: 5967(2007).
16. X. J. Zhang, Q. Li, S.Y. Zhao, C. X. Gao and Z. G. Zhang, J. Sol-gel Sci. Tech. 47: 107(2008).
17. X. J. Zhang, S. Y. Zhao, C. X. Gao and S. J. Wang, J. Sol-Gel Sci. Technol. 49: 221(2009).
18. X. J. Zhang, Y. H. Gao, B. Y. Ren and N. Tsubaki, J. Mater. Sci. DOI 10.1007/s10853-009-4138-8.
19. B. E. Yoldas, Ceram. Bull. 54: 289(1975).
20. P. Sarrazin and C. Coddet, Corros. Sci. 14: 83(1974).
21. I. Barin, Thermochemical Data of Pure Substrates, VCH, Weinheim, (1989).
22. M. Zhu, M. S. Li, Y. L. Li and Y. C. Zhou, Mater. Sci. Eng. A 415:177(2006).